

Formation of a *Cmcm* phase in SnS at high pressure; an *ab initio* constant pressure study

Sebahaddin Alptekin^a, Murat Durandurdu^{b,c,*}

^a Fizik Bölümü, Çankırı Karatekin Üniversitesi, Çankırı, 18100, Turkey

^b Department of Physics, University of Texas at El Paso, El Paso, TX 79968, USA

^c Fizik Bölümü, Ahi Evran Üniversitesi, Kırşehir, 40100, Turkey

ARTICLE INFO

Article history:

Received 23 November 2009

Received in revised form

9 January 2010

Accepted 2 February 2010

by S. Miyashita

Available online 7 February 2010

Keywords:

A. Semiconductors

C. Phase transformation

ABSTRACT

The stability of SnS at high pressure is studied using a constant pressure *ab initio* technique. For the first time, a pressure-induced phase transformation from the *Pnma* structure to a *Cmcm* structure with the application of pressure is predicted through the simulations in this material. The *Cmcm* phase is still a layered structure, consisting of rocksalt-like bilayers, similar to that formed at high temperatures. The *Cmcm* structure is fivefold coordinated. This phase transformation gradually proceeds and is due to the significant decrease of the second neighbor distances. This phase change is also studied by total energy calculations.

© 2010 Elsevier Ltd. All rights reserved.

1. Introduction

Two dimensional layered group IV–VI compounds have various potential applications in optoelectronic devices because of their remarkable electronic and optical properties. Therefore, in the past few years, much effort has been devoted to understanding their physical properties and pressure-induced phase transitions [1–8]. However, there are still unknowns and controversies about the presence or absence of the phase transitions in some of these compounds. The origin of these controversies is not clear, but possibly related to the sample's properties, the pressurizing techniques and the degree of hydrostatic pressure.

Among two dimensional layered group IV–VI compounds, SnS has a layered orthorhombic structure with the *Pnma* space group. The unit cell consists of two layers, and atoms within the layers are covalently bonded to three neighbors (see Fig. 1). The layers pile up with a weak van der Waals-like coupling along *a*-direction. At high temperatures, SnS (α -SnS) undergoes a second order phase transformation from the *Pnma* structure to a more symmetric β -SnS having a *Cmcm* symmetry [9,10]. In the β -SnS state, the atoms also form double layers but each atom in β -SnS is fivefold coordinated. At high pressures, α -SnS transforms into a monoclinic phase (γ -SnS) at 18.15 GPa with a large volume change [11].

Unfortunately, the crystal structure of the high-pressure phase (γ -SnS) and its atomic positions could not be solved in the experiment. Furthermore, in the same study [11], *ab initio* calculations were performed to solve the atomic structure of the high pressure phase of SnS but the calculations were unsuccessful.

The limited information about the high pressure phase of SnS stimulates us to explore its behavior under hydrostatic pressure using an *ab initio* constant pressure technique. For the first time, a gradual phase transformation from α -SnS to β -SnS at high pressure is predicted through the simulation. Our findings might offer the opportunity to better understand the behavior of SnS and the other two dimensional layered structures under pressure.

2. Methodology

We used the first-principles pseudopotential method within the density functional theory (DFT) and the generalized gradient approximation (GGA) of Perdew–Burke and Ernzerhof for the exchange–correlation energy [12]. The calculation was carried out with the *ab initio* program SIESTA [13] using a linear combination of atomic orbitals as the basis set, and the norm-conservative Troullier–Martins Pseudopotentials [14]. Double- ξ plus polarized basis sets were employed. A uniform mesh with a plane wave cut-off of 150 Ry was used to represent the electron density, the local part of the pseudopotentials, and the Hartree and the exchange–correlation potential. The simulation cell consists of 96 atoms with periodic boundary conditions. We used Γ -point sampling for the Brillouin zone integration. The system was first

* Corresponding author at: Department of Physics, University of Texas at El Paso, El Paso, TX 79968, USA.

E-mail address: mdurandurdu@utep.edu (M. Durandurdu).

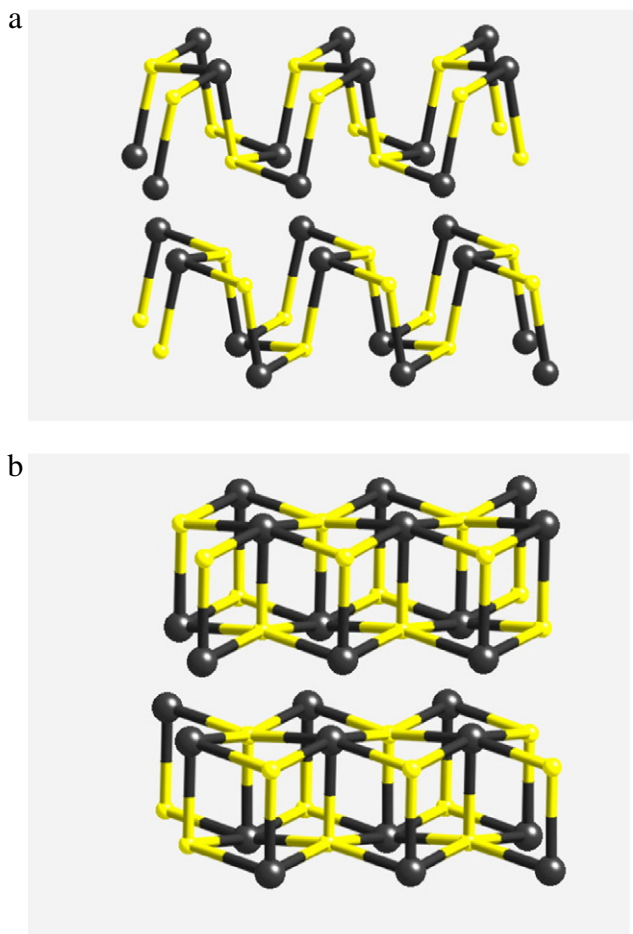


Fig. 1. Crystal structures of SnS (a) the *Pnma* phase at zero-pressure and (b) the *Cmcm* phase of SnS formed at 15 GPa. For clarity, a small portion of the simulation cell is shown.

equilibrated at zero pressure, and then pressure was gradually increased. For each value of the applied pressure, the structure was allowed to relax and find its equilibrium volume and the lowest-energy by optimizing its lattice vectors and atomic positions together until the stress tolerance was less than 0.5 GPa and the maximum atomic force was smaller than 0.01 eV \AA^{-1} . For the minimization of geometries, a variable-cell shape conjugate-gradient method under a constant pressure was used. For the energy volume calculations, we considered the unit cell for SnS phases. The Brillouin zone integration was performed with an automatically generated $10 \times 10 \times 10$ *k*-point mesh for the phases following the convention of Monkhorst and Pack [15]. In order to determine the symmetry of the high pressure phases formed in the simulations, we used the KPLLOT program [16] that provides detailed information about the space group, the cell parameters and the atomic position of a given structure. For the symmetry analysis we used 0.2 \AA , 4° , and 0.7 \AA tolerances for the bond lengths, the bond angles and the interplanar spacing, respectively.

In the previous investigation on GeS [8], isostructural to SnS, an approximate *ab initio* technique (a non-self-consistent version of the DFT based on the linearization of the Kohn–Sham equation by a Harris functional approximation [17]) within a local density approximation was used to predict the high pressure phase of GeS. The use of the Harris functional however might raise some concerns about the accuracy of the calculations, in contrast to the self-consistent calculations. Additionally, relative to the local density approximations, the generalized gradient approximations more correctly describe the relative energy difference between the

phases and hence the critical pressure, see for example Ref. [21]. Therefore in this study we adopted the self consistent calculation and a generalized gradient approximation to eliminate any doubt about the accuracy of our data and to confirm our prediction in GeS.

3. Constant pressure *ab initio* simulation

For the *Pnma* phase of SnS, we first compare our calculated lattice parameters with the available experimental data [11]. The equilibrium unit cell lattice constants of SnS are found to be $a = 11.34 \text{ \AA}$, $b = 4.03 \text{ \AA}$ and $c = 4.35 \text{ \AA}$. These values are comparable with the experimental results of $a = 11.20 \text{ \AA}$, $b = 3.98 \text{ \AA}$ and $c = 4.33 \text{ \AA}$ [11]. The SnS structure has two distinct bond lengths of 2.68 \AA and 2.70 \AA at ambient pressure. These values are in agreement with the experimental results of 2.627 \AA – 2.665 \AA [11]. The nearest nonbonding distance between atoms in different layers is 3.299 \AA . The experimental value of this separation is 3.290 \AA [11].

Starting from the zero-pressure structure, we gradually increase pressure and carefully analyze the structure of SnS at each applied pressure using the KPLLOT program. At 15 GPa, we find a phase transformation into an orthorhombic structure with a space group *Cmcm* having eight atoms per unit cell. The *Cmcm* crystal at 15 GPa is illustrated in Fig. 1. Its lattice parameters are $a = 3.519 \text{ \AA}$, $b = 10.82 \text{ \AA}$ and $c = 4.15 \text{ \AA}$ and its atomic positions are Sn: (0, 0.88551, 0.25) and S: (0, 0.643331, 0.25). This high-pressure phase has a layer-like structure and resembles to a CrB-type phase. The structure consists of rocksalt-like bilayers, stacked along the *b* axis of the orthorhombic unit cell. Each Sn and S atom has five unlike neighbors but the Sn–S separations do not have the same bond lengths on all sites. Both Sn and S have four neighbors at 2.74 \AA in the *b*–*c* planes and one neighbor at 2.62 \AA perpendicular to the layer planes. The closest Sn–Sn and S–S neighbor separations are about 3.23 \AA and 3.57 \AA , respectively.

The variation of the simulation cell vectors as a function of pressure might provide valuable information about this phase transformation at the atomistic level. Fig. 2 shows the cell lengths as a function of the applied pressure. As can be seen from the figure, the SnS structure exhibits a strong anisotropic compression. The *c*-axis is found to be more compressible than the other axes even though the *a*-direction is perpendicular to the layers. This implies that the main compression mechanism of SnS is due to the significant shortening along the puckered layers, similar to what has been observed in isostructural GeS [3,8] and GeSe [2,4]. This trend, however, is quite different from the other layer-like chalcogenides such as SnS_2 [18] and TiS_2 [19] in which the strongest compression occurs along the weak interlayer direction. It is also noteworthy here that the simulation cell angles remain 90° during the phase transformation and hence this phase change is not associated with the shear deformation.

To investigate the structural changes through the transition further, we study the variation of the first neighbor Sn–S bond lengths under pressure. The SnS structure has two distinct bond lengths at ambient pressure. The bonds, nearly parallel with the *a* axis, have an average value of 2.7 \AA and those in the *b*–*c* planes are 2.68 \AA at zero pressure. Both Sn–S separations as a function of pressure are depicted in Fig. 3. As can be clearly seen from the figure, the bonds, nearly parallel with the *a*-axis, are found to be more sensitive to pressure than those in the *b*–*c* planes and they gradually decrease. The bonds in the *b*–*c* planes initially decrease but owing to the phase transformation, they suddenly increase. The change of the bond lengths is less than 2%. With increasing pressure, the bond angles also decrease (around 3%–4%), indicating the occurrence of bond bending in the structure. We also study the closest nonbonding separations in all directions and plot their pressure dependence in Fig. 4. The Sn–S distances, roughly along the *a*-axis and in the *b*–*c* planes, might be

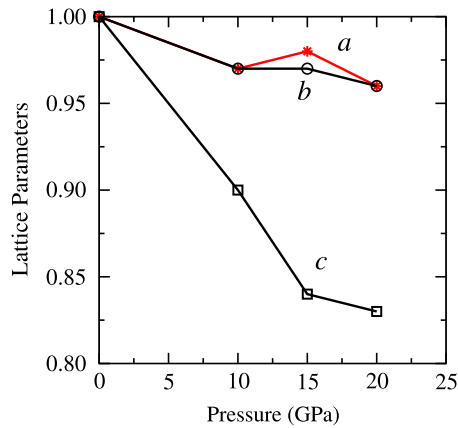


Fig. 2. Variation of the simulation cell lengths as a function of pressure.

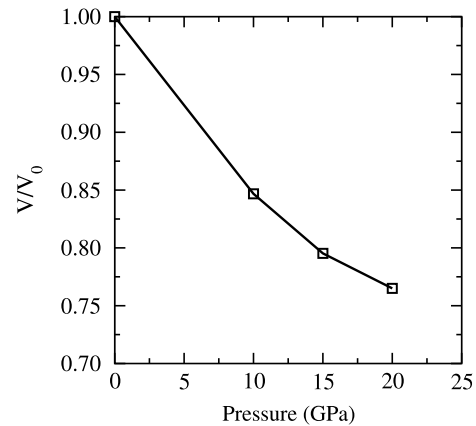


Fig. 5. Pressure–volume relation.

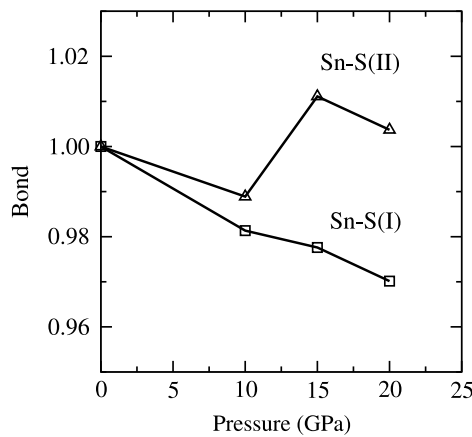


Fig. 3. The first neighbor Sn–S distances (Sn–S(I) denotes the bond length, nearly parallel with the *a*-axis, Sn–S(II) denotes the bond length in the *b*–*c* planes).

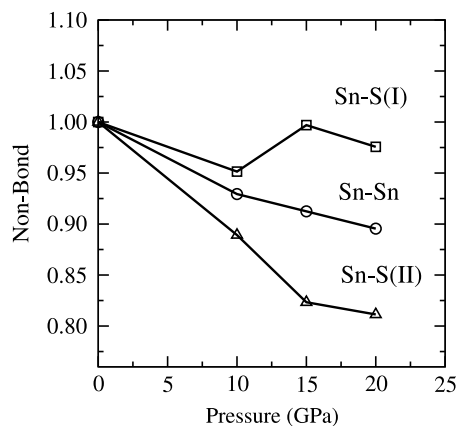


Fig. 4. Nonbonding closest separation The distance nearly parallel with the *a*-axis is referred to as Sn–S(I). The separation in the *b*–*c* planes is represented by Sn–S(II). The nonbonding length along the *b*-axis is denoted by Sn–Sn.

considered as an interlayer and an intralayer spacing, respectively. The Sn–S nonbonding separations in the *b*–*c* planes are remarkably shortened, relative to the others. From these observations, we conclude that the major compression mechanism of SnS is due to the narrowing of the intralayer and interlayer separations and the bond bending.

Fig. 5 shows the pressure volume relation. As can be seen from the figure, the structural phase transition in SnS proceeds gradually as in the temperature-induced phase transformation in SnS.

4. Enthalpy calculations

Transition pressures predicted in constant-pressure simulations are generally overestimated, in analogy to superheating molecular-dynamics simulations. This implies a high intrinsic activation barrier for transforming one solid phase into another in simulations. When the particular conditions such as finite size of simulation cells and the lack of any defects and surfaces in the simulated structures are considered, such overestimated transition pressures are anticipated. Structural phase transformations in the simulations do not proceed by nucleation and growth, but instead they occur across the entire simulation cells. As a result, the systems have to cross a significant energy barrier to transform from one phase to another one, and hence the simulated structures have to be overpressurized in order to obtain a phase transition. Additionally the absence of the thermal motion (relaxation of the structure at constant pressure) in our simulation shifts the phase transformation to a higher pressure. On the other hand, the thermodynamic theorem does not take into account the possible existence of such an activation barrier separating the two structural phases and the thermal motion. Therefore as a next step, we consider the energy–volume calculations to study the stability of the *Cmcm* and *Pnma* phases. Each structure was equilibrated at several volumes and their energy–volume relations were fitted to the third-order Birch Murnaghan equation of states. The energy–volume curve of the structures is presented in Fig. 6. Accordingly, the energies of the *Pnma* and *Cmcm* crystals overlap one another after a certain volume. This behavior is comparable with a continuous phase transition between these structures, which is also clearly reflected in the enthalpy calculation (see below). This finding validates our constant-pressure *ab initio* simulation.

The transition pressure between the *Pnma* state and the *Cmcm* state is determined by a simple comparison of their static lattice enthalpies $H = E_{tot} + pV$. The crossing of two enthalpy curves indicates a pressure-induced phase transition between these two phases. The computed enthalpy curve of the *Pnma* and *Cmcm* phases is plotted as a function of pressure in Fig. 7. The curves cross around 4.5 GPa. However, the enthalpy of both phases above 4.5 GPa has practically the same values and it is impossible to distinguish which structure is more stable than the other. This again provides a clear evidence of a gradual phase transition between *Pnma* and *Cmcm*. The *Pnma* and *Cmcm* phase change is expected to occur around 4.5 GPa in experiments.

From the energy–volume data, we also calculate the bulk modulus of these phases. For the *Pnma* state, our bulk modulus is 38.27 GPa, which is in good agreement with the experimental value of 36.6 GPa [11] and the theoretical value of 39.55 GPa [20]. The bulk modulus of the *Cmcm* phase is predicted to be 46.51 GPa.

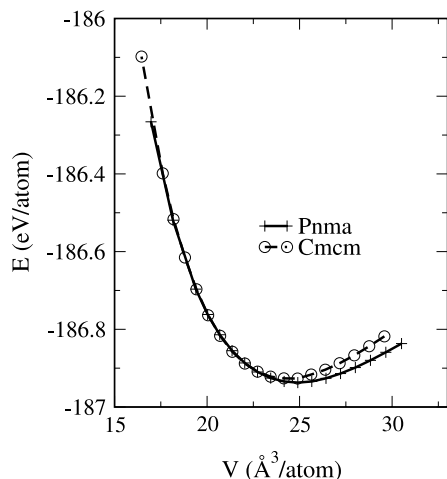


Fig. 6. Energy volume curve of *Pnma* and *Cmc* phases.

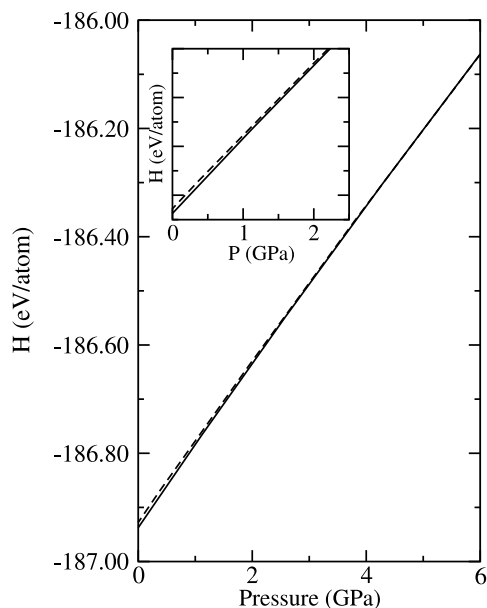


Fig. 7. Enthalpy curve of *Pnma* (solid line) and *Cmc* (dashed line). The curves cross around 4.5 GPa.

5. Discussion

Our simulations show the existence of the α -SnS to β -SnS phase transformation at high pressures. Such a phase transformation in SnS also takes place a temperature of about 878 K. At 905 K, the lattice constants of the high temperature *Cmc* phase are $a = 4.148 \text{ \AA}$, $b = 11.48 \text{ \AA}$ and $c = 4.177 \text{ \AA}$ [10]. The bond lengths in the plane of the slabs are equal to 2.96 \AA and the interlayer Sn–S bond length perpendicular the plane of slabs is 2.63 \AA [10]. It is noteworthy here that the lattice constants and the bond lengths of the high temperature *Cmc* phase are comparable with those of the *Cmc* phase formed at high pressure in the present study, indicating that both phases have a similar atomic structure. It is indeed unsurprising to see the formation of a fivefold-coordinated *Cmc* phase in SnS under pressure because of its unique structure in which there are only two next unlike nearest neighbors at a certain distance. With increasing pressure, each atom forms a bond with these neighbors, and the threefold-coordinated phase transforms into a fivefold-coordinated *Cmc* state. However, this phase change has not been observed in experiments and α -SnS directly transforms into a monoclinic phase at 18.15 GPa [11]. The origin

of the contradictory observation in the present study and that experiment is not clear but might be due to some factors that might limit obtaining any meaningful data or the correct interpretations for the high pressure phase of SnS. The controversy might be associated with the misinterpretation of the diffraction patterns in the experiment. It is also possible that the sample properties might favor the formation of the monoclinic or orthorhombic *Cmc* phases in SnS. Samples used experiments have defects (impurities, vacancies etc) while the simulated structures are defect free. The degree of hydrostatic pressure is another factor that might be responsible for the contradictory observation since the layered structures are very sensitive to shear deformations. The degree of the hydrostaticity in experiments is determined by the efficiency of the pressure-transmitting medium. At high pressures, the pressure-transmitting medium solidifies resulting in strong nonhydrostatic effects. Even in the low pressure regime, the pressure in the diamond anvil cell is not exactly hydrostatic. On the other hand, perfect hydrostatic pressure can be always preserved in simulations. Finally we have to underline here that in the experimental paper [11], *ab initio* calculations were also used to understand the high pressure phase of SnS and the mechanism of the α -SnS to γ -SnS phase transformation but all attempts to prove the high pressure phase of SnS and the transformation mechanism were unsuccessful.

In the previous investigation on GeS [8], isostructural to SnS, we also observed the formation of the fivefold coordinated orthorhombic *Cmc* phase at high pressures. Furthermore, the *Pnma* to *Cmc* transformation mechanism of GeS [8] is reported to be similar to what has been observed in SnS. The observations of very similar behaviors (the high pressure phase and the transformation mechanism) in SnS and GeS using very different theoretical methodologies are particularly important because they hopefully eliminate any concern about the prediction of a high pressure phase of GeS and its transformation mechanism [8]. Moreover, these similar behaviors might suggest that the *Pnma* to *Cmc* phase transformation can be induced in GeS at high temperatures as well and this phase transformation can be generic in the group IV–VI compounds because SnSe also undergoes the same phase transformation at high temperatures [9]. Certainly, further experimental and theoretical studies are needed to have a generally accepted picture about the behaviors of these compounds at high temperatures and pressures.

6. Conclusions

We have used an *ab initio* constant pressure technique within a generalized gradient approximation to study the pressure-induced phase transition in SnS and predicted a gradual phase transformation from the threefold coordinated orthorhombic structure to a fivefold coordinated orthorhombic structure (*Cmc*). This phase is similar to the phase formed in SnS at high temperatures. We also provide substantial information about the *Pnma*-to-*Cmc* phase transformation at the atomistic level. This phase change is also studied by total energy calculations and expected to occur around 4.5 GPa in experiments.

Acknowledgement

The visit of MD to Ahi Evran Üniversitesi was supported by the Scientific and Technical Research Council of Turkey (TÜBİTAK) BİDEB-2221.

References

- [1] K.L. Bhatia, G. Parthasarathy, D.P. Gosain, E.S.R. Gopal, Phys. Rev. B 33 (1986) 1492.
- [2] H.C. Hsueh, H. Vass, S.J. Clark, G.J. Ackland, J. Crain, Phys. Rev. B 51 (1995) 16750.

- [3] H.C. Hsueh, W.C. Warren, H. Vass, G.J. Ackland, S.J. Clark, J. Crain, *Phys. Rev. B* 53 (1996) 14806.
- [4] A. Onodera, I. Sakamoto, Y. Fujii, N. Mori, S. Sugai, *Phys. Rev. B* 56 (1997) 7935.
- [5] T. Chattopadhyay, A. Werner, H.G. von Schnering, in: C. Homan, R.K. MacCrone, E. Whalley (Eds.), *High Pressure in Science and Technology*, MRS Symposia Proceedings No. 22, (Materials Research Society, Pittsburgh, 1984), p. 83.
- [6] K.G. Khvostantzev, V.A. Sidorov, *Phys. Status Solidi B* 116 (1983) 83.
- [7] A.M. Redon, J.M. Leger, *High Press. Res.* 4 (1990) 315.
- [8] M. Durandurdu, *Phys. Rev. B* 72 (2005) 144106.
- [9] H. Wiedemeir, F.J. Csillag, *Z. Kristallogr.* 149 (1979) 17.
- [10] H.G. von Schnering, H.Z. Wiedemeir, *Z. Kristallogr.* 156 (1981) 143.
- [11] L. Ehm L., K. Knorr, P. Dera, A. Krimmel, P. Bouvier, M. Mezouar, *J. Phys. Condens. Matter* 16 (2004) 3545. 2004.
- [12] J.P. Perdew, K. Burke, M. Ernzerhof, *Phys. Rev. Lett.* 77 (1996) 3865.
- [13] P. Ordejón, E. Artacho, J.M. Soler, *Phys. Rev. B* 53 (1996) 10441.
- [14] N. Troullier, J.M. Martins, *Phys. Rev. B* 43 (1991) 1993.
- [15] H.J. Monkhorst, J.D. Pack, *Phys. Rev. B* 13 (1976) 5188.
- [16] R. Hundt, J.C. Schön, A. Hannemann, M. Jansen, *J. Appl. Crystallogr.* 32 (1999) 413.
- [17] J. Harris, *Phys. Rev. B* 31 (1985) 1770.
- [18] K. Knorr, L. Ehm, M. Hytha, B. Winkler, W. Depmeier, *Phys. Status Solidi B* 223 (2001) 435.
- [19] D.R. Allan, A.A. Kelsey, S.J. Clark, R.J. Angel, G.J. Ackland, *Phys. Rev. B* 57 (1998) 5106.
- [20] M. Rajagopalan, G. Kalpana, V. Priyamvadha, *Bull. Mater. Sci.* 29 (2006) 25.
- [21] M. Fuentes-Cabrera, H. Wang, O.F. Sankey, *J. Phys.: Condens. Matter* 14 (2002) 9589.